Heliyon 10 (2024) e27710

Contents lists available at ScienceDirect

Heliyon

journal homepage: www.cell.com/heliyon

Research article

Identification of prognostic models for glycosylation-related subtypes and tumor microenvironment infiltration characteristics in clear cell renal cell cancer

Cheng Shen [a,b,1], Bing Zheng [a,1], Zhan Chen [a,b,1], Wei Zhang [a], Xinfeng Chen [a], Siyang Xu [c], Jianfeng Ji [d], Xingxing Fang [e,**], Chunmei Shi [a,*]

[a] Department of Urology, Affiliated Hospital 2 of Nantong University, China
[b] Medical Research Center, Affiliated Hospital 2 of Nantong University, China
[c] Clinical Medicine Specialty, Xinglin College of Nantong University, China
[d] Department of Burn and plastic surgery, Affiliated Hospital 2 of Nantong University, China
[e] Nephrology Department, Affiliated Hospital 2 of Nantong University, China

ARTICLE INFO

Keywords:
Renal clear cell carcinoma
Glycosylation-related genes (GRGs)
Immune infiltration
Signature
Molecule subtypes

ABSTRACT :

Background: One of the most fatal forms of cancer of the urinary system, renal cell carcinoma (RCC), significantly negatively impacts human health. Recent research reveals that abnormal glycosylation contributes to the growth and spread of tumors. However, there is no information on the function of genes related to glycosylation in RCC.

Methods: In this study, we created a technique that can be used to guide the choice of immunotherapy and chemotherapy regimens for RCC patients while predicting their survival prognosis. The Cancer Genome Atlas (TCGA) provided us with patient information, while the GeneCards database allowed us to collect genes involved in glycosylation. GSE29609 was used as external validation to assess the accuracy of prognostic models. The "ConsensusClusterPlus" program created molecular subtypes based on genes relevant to glycosylation discovered using differential expression analysis and univariate Cox analysis. We examined immune cell infiltration as measured by estimate, CIBERSORT, TIMER, and ssGSEA algorithms, Tumor Immune Dysfunction and Exclusion (TIDE) and exclusion of tumour stemness indices (TSIs) based on glycosylation-related molecular subtypes and risk profiles. Stratification, somatic mutation, nomogram creation, and chemotherapy response prediction were carried out based on risk factors.

Results: We built and verified 16 gene signatures associated with the prognosis of ccRCC patients, which are independent prognostic variables, and identified glycosylation-related genes by bioinformatics research. Cluster 2 is associated with lower human leukocyte antigen expression, worse overall survival, higher immunological checkpoints, and higher immune escape scores. In addition, cluster 2 had significantly better angiogenic activity, mesenchymal EMT, and stem ability scores. Higher immune checkpoint genes and human leukocyte antigens are associated with lower overall survival and a higher risk score. Higher estimated and immune scores, lesser tumor purity, lower mesenchymal EMT, and higher stem scores were all characteristics of the

* Corresponding author. Department of Urology, Affiliated Hospital 2 of Nantong University, 226001, China.
** Corresponding author. Nephrology Department, Affiliated Hospital 2 of Nantong University, 226001, China.
E-mail addresses: 48776592@qq.com (X. Fang), 1340726198@qq.com (C. Shi).
[1] These authors contributed equally to this work.

https://doi.org/10.1016/j.heliyon.2024.e27710
Received 13 October 2023; Received in revised form 4 March 2024; Accepted 5 March 2024
Available online 13 March 2024

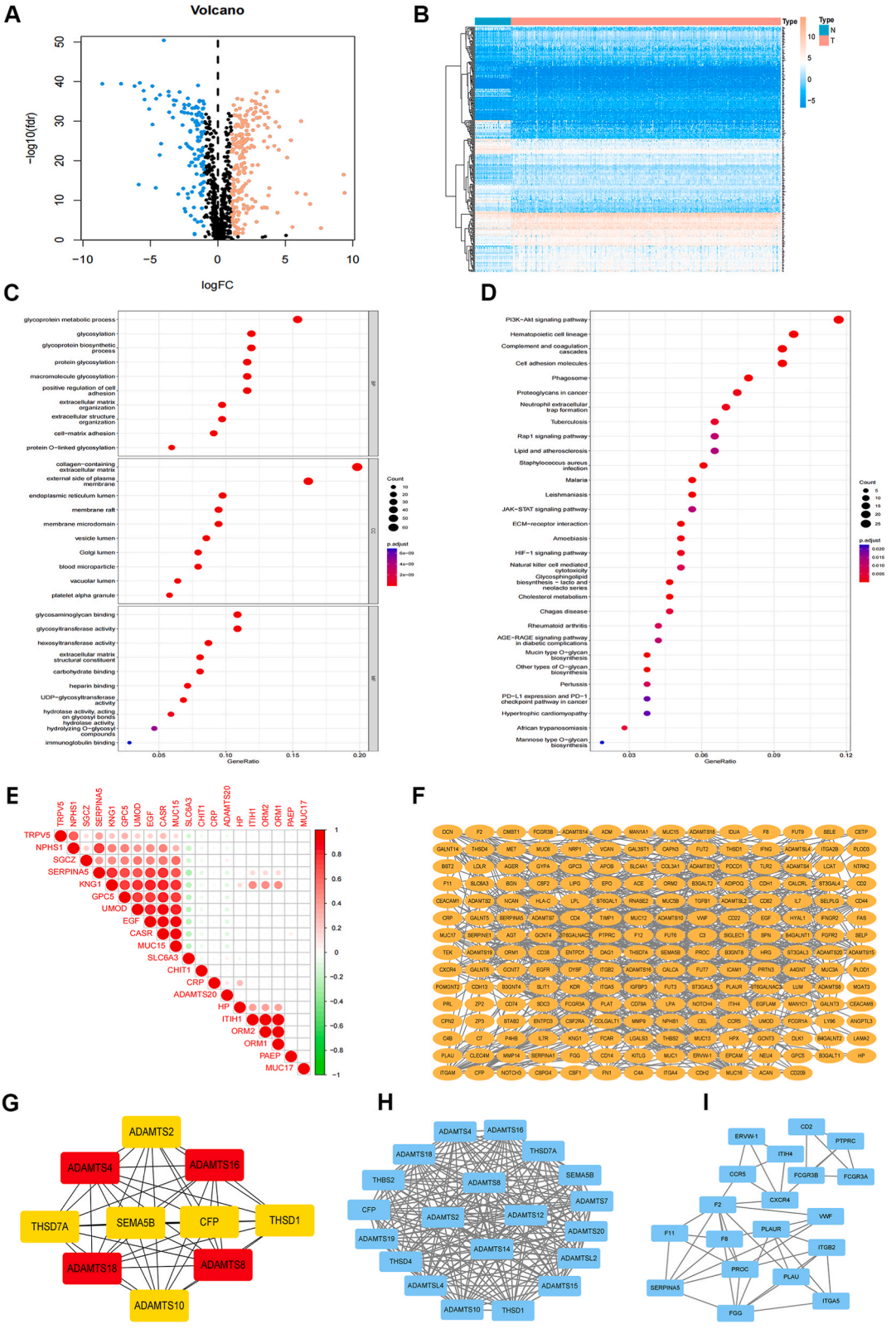

(caption on next page)

Fig. 1. | (A) 209 up-regulated and 122 down-regulated GRGs in the ccRCC are depicted on a volcano plot (FDR 0.05 and |logFC| > 1). (B) Heatmap of 331 DE-GRGs between normal kidney and ccRCC tissues. (C) For DE-GRGs, the top ten enriched phrases according to GO analysis belonged to BP, CC, and MF. (D) The top thirty enriched terms in KEGG analysis. (E) The correlations between the top ten up-regulated and down-regulated GRGs. (F) According to the STRING database, PPI network of the DE-GRGs. (G) The hub genes found using the "cytohubba" plugin (H, I) Two modules that were acquired using the "MCODE" plugin. CcRCC, clear cell renal cell cancer; GRGs, or glycosylation-related genes; FDR, or false discovery rate; FC, or fold change; DE-GRGs, differentially expressed GRGs; Gene Ontology, biological process, cell component, and molecular function are abbreviations for these terms. Kyoto Encyclopedia of Genes and Genomes, or KEGG; Protein-protein interaction, or PPI.

high-risk group. High amounts of tumor-infiltrating lymphocytes, a high mutation load, and a high copy number alteration frequency were present in the high-risk group.
Discussion.
According to our research, the 16-gene prognostic signature may be helpful in predicting prognosis and developing individualized treatments for patients with renal clear cell carcinoma, which may result in new personalized management options for these patients.

1. Introduction

The cancer of the urinary system with the greatest frequency, renal cell carcinoma (RCC), is characterized by high-grade malignancies [1]. RCC can be broadly classified into three subgroups based on morphology: suspicious cell malignancies, clear cell renal cell cancer (ccRCC), and Kidney renal papillary cell carcinoma. More than 70% of RCC patients are kidney renal clear cell carcinoma (KIRC) instances [2]. Despite improvements in treatment methods, only 12% of individuals with clear cell renal cell carcinoma (ccRCC) have 5-year overall survival rates (OS) [2,3]. The prognosis of most patients remains dismal despite substantial improvements in diagnostic procedures and targeted therapy. The importance of genetic indicators in the highly individualized, precision medicine age is being supported by more and more data [4,5]. Finding biomarkers that aid in predicting the propensity for relapse and mortality is crucial for clinical decision-making and treatment targeting.

The tumor microenvironment (TME) is crucial in the development of tumor. TME comprises various cell types, such as vascular cells, cancer-associated fibroblasts, invading immune cells, etc. These cells can regulate angiogenesis, tumor cell invasion, growth inhibitory factor evasion, energy metabolism, immune evasion, and cell proliferation and death in a cell-involuntary way [6]. Emerging research indicates that modifications in glycosylation mediated by the tumor microenvironment have essential functional roles in tumor growth and metastasis, including cell adhesion, motility, invasion, and immune evasion. These changes in glycosylation are similar to oncogene activation and tumor suppressor gene loss, which are hallmarks of tumor formation [7–9]. Additionally, data show that genes related to glycosylation are linked to immune infiltration, expression of the programmed cell death ligand 1 (PD-L1), and head and neck squamous cell carcinoma (HNSCC) diagnosis and targeted treatment [10]. However, there is no information on the function of genes associated with glycosylation in ccRCC.

In this research, we used differential expression analysis, univariate and multivariate Cox regression, and 16 glycosylation-related genes (GRGs) to independently assess the prognosis of ccRCC using the Cancer Genome Atlas (TCGA) database. Additionally, we looked into nomogram creation, somatic mutation analysis, and the prediction of chemotherapeutic response.

2. Results

2.1. Identification of genes involved in differential glycosylation and analysis of biological function

One thousand-five genes associated with glycosylation were found in the GeneCards database, and protein-coding genes and correlation values higher than two were used as screening standards. Supplementary fig. S1 depicts the study's primary flow. After that, by comparing kidney tissue from ccRCC with normal kidney tissue, a differential analysis revealed 209 upregulated and 122 downregulated genes (Fig. 1A and B). According to GO and KEGG pathway enrichment studies, the following differentially expressed genes were primarily enriched in proteoglycans, cell adhesion molecules, biological processes connected to tumors, and signaling pathways in immunity and cancer (Fig. 1C and D). The top 10 up-and-down-regulated genes and their correlations are also displayed (Fig. 1E). PPI networks were investigated in the STRING database and shown in Cytoscape (Fig. 1F). The top 10 hub genes were sorted (Fig. 1G), and two modules were discovered using MCODE (Fig. 1H and I).

2.2. Identification of glycosylation-related clusters and correlation analysis between clusters and tumor immune microenvironment, tumorigenesis score, and TSIs

We identified 41 genes linked with prognosis by univariate Cox analysis, of which 15 genes (BTD, ST6GALNAC3, MYORG, CDH13, ABCG2, PKHD1, TEK, FUT6, TLR3, KL, DYSF, CALCRL, PODXL, CAT, KDR) were protective factors and 26 genes were risk factors (Fig. 2A). Most of the genes were shown to be associated using correlation analysis (Fig. 2B). According to a further clustering study using 41 prognosis-related genes, ccRCC patients are best classified when split into two categories (Fig. 2C). The survival study of the two subgroups of ccRCC patients revealed that cluster 1 had a better prognosis than cluster 2. (Fig. 2D).

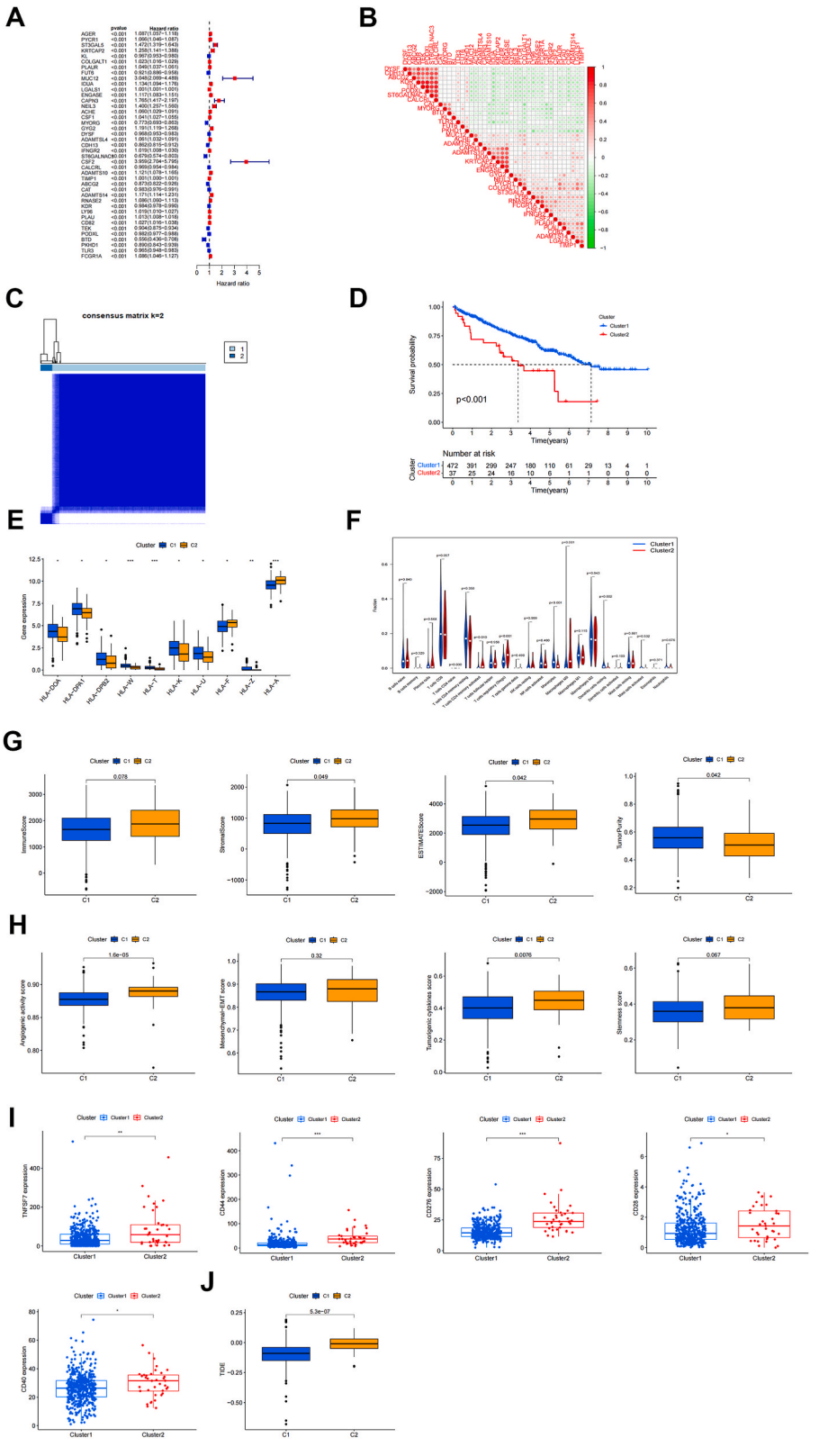

(caption on next page)

Fig. 2. | (A) Ten DE-GRGs connected to prognosis were shown using a univariate Cox analysis. (B) The correlations between the ten genes. (C) Clustering consensus matrix for k = 2. (D) The survival difference between clusters 1 and 2 is represented by the KM curve. The expression of MHC molecules (E), immune cell infiltration using CIBERSORT (F), immune and stromal scores using ESTIMATE (G), angiogenic activity, mesenchymal-EMT, tumourigenic cytokines and stemness scores (H), five common immunoinhibitors (I), and TIDE score (J) between the two clusters. CDF, Cumulative distribution function; KM, Kaplan–Meier; EMT, Epithelial-mesenchymal-transition; TIDE, Tumour Immune Dysfunction and Exclusion.

Additionally, we discovered that cluster 2 was linked to the poor expression of several MHC molecules (Fig. 2E). Further analysis using the CIBERSORT algorithm revealed that Cluster 2 was linked to more significant immune cell infiltration, including T cells CD4 memory activated, T cells CD4 naïve, monocytes, macrophages M0, and T regulatory cells (Tregs) (Fig. 2F). The estimate method revealed that Cluster 2 had reduced tumor purity and higher stromal and estimate scores (Fig. 2G). Additionally, Cluster 2 had considerably more significant levels of angiogenic activity and tumorigenic cytokines (Fig. 2H).

We examined the relationship with immunological checkpoints since there were substantial variations between the two groups regarding immune infiltration. Cluster 2 had increased levels of CD28, CD40, CD44, CD276, and TNFRSF7 expression (Fig. 2I). Higher TIDE scores were linked to Cluster 2 (Fig. 2J).

2.3. Establishment and validation of glycosylation related prognostic models

We used multivariate Cox regression to further screen the model's gene set, ultimately adding 16 genes to the signature (Fig. 3A). Fig. 3B displays the coefficients for each gene in the signature. The relationship between the risk score and the hallmark genes is shown in Fig. 3C. With a 1-year AUC of 0.794, patients with a high-risk score had a poorer prognosis than those with a low-risk score (Fig. 3D). Results of survival analysis were validated in GSE29609 dataset (Fig. 3E). According to empirical research, patients in the high-risk group fared worse than those in the low-risk group, and these differences were present across virtually all clinical groupings (Supplementary fig. S2). Additionally, univariate and multivariate Cox regression analysis revealed that signature was a separate risk factor (Fig. 3F and G). Finally, we looked at variations in risk ratings across subgroups based on several clinicopathological criteria. The findings demonstrated that patients with T3-4 stage, Grade 3–4, and Stage III-IV had higher risk scores, indicating that the more advanced the tumor, the higher the risk score (Fig. 3H–J).

Based on the aforementioned multiple Cox regression analysis outcomes, we took age and signature into account while building a nomogram, with signature being the most crucial component (Fig. 3K). Actual survival times of 1, 3 and 5 years were extremely compatible with anticipated survival durations, according to calibration plots (Fig. 3L). In addition, we constructed a nomogram by integrating prognostic models from externally validated datasets and clinical factors selected by univariate and multivariate Cox regression analyses (Fig. 3M).

2.4. Comparison of gene expression-based prognostic features in renal clear cell carcinoma

Significant machine-learning-based prognostic and predictive gene expression signatures have been created in recent years thanks to advances in next-generation sequencing and big data technology [11]. We thoroughly searched the published signatures of ccRCC to compare the performance of GRGs with other signatures. There were six registered signatures [12–17](Supplementary table 1). The biological processes of pyroptosis, iron death, RNA-binding proteins, necroptosis, WNT, and drug sensitivity are all linked to these characteristics. Based on time-dependent ROC for ccRCC, we examined all models to forecast predictive effects. Our model outperforms other models, and we found that while most models performed well on their training datasets, they performed severely on external datasets, likely owing to poor model generality brought on by overfitting.

2.5. Tumor immune cell infiltration and immune checkpoint inhibitors were estimated based on characteristics

We used GSEA to examine possible pathways to control tumorigenesis in the high-risk group. The findings revealed that the high-risk group had considerable enrichment in the P53 pathway (NES = 1.84, NOM p-value = 0.02, FDR q-value = 0.148) and numerous other traditional tumor-associated pathways (Fig. 4A). With NES = 1.67, NOM p-value = 0.008, and FDR q-value = 0.169, the VEGF signaling pathway was deemed the most pertinent KEGG signaling pathway (Fig. 4B).

Previous research has demonstrated that the tumor microenvironment is crucial to the formation of tumors [18]. Using GSEA, we initially discovered that several immune-related pathways were linked to high-risk groups (Fig. 4C). We thus looked at the connection between this characteristic and the tumor immune microenvironment. According to the ssGSEA algorithm, high-risk groups had more immune-related activities or pathways and more immune cell infiltration than low-risk groups (Fig. 4D). The ESTIMATE algorithm looked at the statistics above and discovered that the high-risk group had lower tumor purity, higher immunological scores, and estimated scores (Fig. 4E). In the high-risk group, follicular helper T cells, regulatory T cells, CD8 + T cells, and macrophages were the primary immune cells entering the body (Fig. 4F). Dendritic and activated mast cells were also more prevalent in the high-risk group (Fig. 4G). Additionally, we looked at MHC expression and discovered that the high-risk group had a much higher level of MHC expression (Fig. 4H). The high-risk group had high CTLA4, PDCD1, and LAG3 immune checkpoint inhibitor expression levels (Fig. 4I).

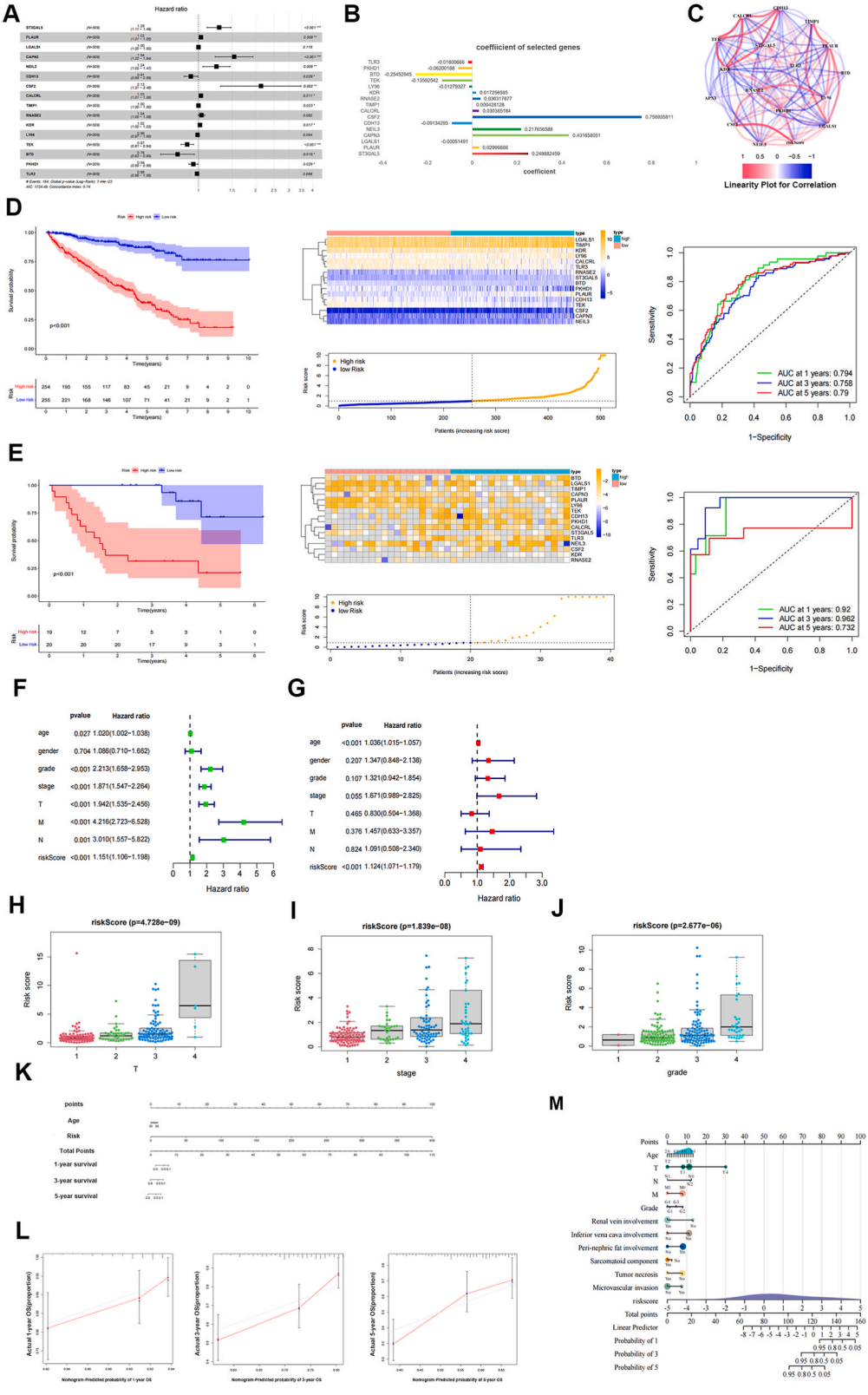

(caption on next page)

Fig. 3. | The 16 genes chosen for the signature by multivariate Cox analysis are depicted in a forest plot in (A). (B) The signature's 16 included genes' coefficients. (C) The relationships between the 16 genes and the signature. ROC analysis, heatmap, and the survival status together with the risk score in the TCGA (D) and GSE29609 cohort (E). Both a univariate (F) and multivariate Cox analysis revealed that the signature was an independent risk factor for ccRCC patients in the TCGA cohort (G). the variations in risk scores across several groups based on clinicopathological characteristics, such as clusters (H), T stage (I), Tumor stage (J), and Tumor grade. (K) Nomogram based on age and risk score. (L) Nomogram calibration plots for forecasting the likelihood of survival for 1, 3, and 5 years. The Cancer Genome Atlas; ROC, receiver operating characteristic.

2.6. Correlation of angiogenic activity, mesenchymal EMT, tumor cytokines, and stemness scores with characteristics

According to earlier research, different clusters were connected to stemness scores, oncoforming cytokines, mesenchymal EMT, and angiogenic activity. We then sought to determine if the processes behind the signature include any of these four tumor-associated activities. In ccRCC patients, we estimated the levels of angiogenic activity, mesenchymal EMT, tumor-promoting cytokines, and stemness. Mesenchymal EMT scores were lower, and tumorigenic cytokine scores were greater in the high-risk group, as shown in Fig. 5A. Fig. 5B displays the relationship between the risk score and four different metrics. It reveals that the risk score was favorably connected with the tumorigenic cytokine score and negatively correlated with the mesenchymal EMT score ($R = -0.19$, $p = 1.9e\text{-}05$). Additionally, TSIs such as EREG-mRNAsi and ENHsi were less common in the high-risk group (Fig. 5C).

2.7. Somatic mutation versus TMB profile

We obtained primary nucleotide variation data from TCGA to examine variations in genomic mutations between high-risk and low-risk groups. The top five genes with the most significant mutation frequency in the high-risk group were VHL (44%), PBRM1 (42%), TTN (15%), SETD2 (15%), and BAP1 (14%), while the top five genes in the low-risk group were VHL (41%), PBRM1 (34%), TTN (16%), SETD2 (8%), and BAP1 (7%) (Fig. 6A and B). Somatic mutation interactions were also found. Most genes had co-existing mutations, and the high-risk group had mutually exclusive SPEN-PBRM1 mutations (Fig. 6C). Additionally, the low-risk group saw frequent gene mutation coexistence (Fig. 6D). Mutation rates in the high-risk group were considerably more significant than in the low-level group when TMB was also compared between the two groups (Fig. 6E). Compared to the high TMB group, the low TMB group's survival time was noticeably longer (Fig. 6F). Using our model, we found that the prognosis of the high-risk + high TMB group was considerably poorer than that of the low-risk + low TMB group (Fig. 6G). Last, we looked at the marker gene's mutation rate and discovered that CSF2 had more amplification mutations, BTD had more deletion mutations, and PKHD1 had more mistranslation mutations (Fig. 6H).

2.8. Chemotherapy response prediction

The two groups' treatment responses to frequently prescribed chemotherapeutic drugs were predicted using GDSC. Between high-risk and low-risk groups, there were substantial differences in the sensitivity to various chemotherapeutic drugs (Fig. 7A). These results may be used to analyze treatment strategies specifically designed for patients in high-risk and low-risk categories. Additionally, the PubChem database was used to display the 3D structures of possible medications (gemcitabine, sorafenib, carmustine, and osimertinib) (Fig. 7B).

2.9. Expression of 16 model genes in ccRCC and adjacent normal tissues

To further validate the expression of model genes, we performed immunohistochemical experiments on clinical ccRCC tissues and normal tissue samples. We observed that nine model genes (ST3GAL5, PLAUR, CAPN3, NEIL3, CSF2, CALCRL, TIMP1, RNASE2, KDR) were more highly expressed in ccRCC than in normal tubular epithelial cells (Fig. 8A), and the remaining seven genes were less expressed in ccRCC compared with adjacent non-cancerous tissues (Fig. 8B). Immunohistochemistry was used to detect the expression of each molecule in three pairs of clinical specimens. This result confirms our analysis of the TCGA dataset.

3. Discussion

Recurrence and metastasis still happen in around 30% of patients with poor clinical outcomes, despite improvements in survival and quality of life brought about by developments in diagnostic methods and thorough treatment. In recent years, several genome-wide biomarkers have been introduced to ccRCC through high-throughput sequencing technologies. For precise prognosis and customized care, they are still insufficient. Increasing evidence suggests that glycosylation-related genes are essential in carcinogenesis, progression, and metastasis of ccRCC. However, no studies focusing on the association of glycosylation-related genes with ccRCC prognostic assessment and molecular subtypes have been published [19,20]. In this work, we discovered a unique glycosylation-related signature made up of 16 genes that may be able to predict a patient's clinical prognosis and response to chemotherapy. Our research may help ccRCC patients receive more accurate survival probability predictions.

In the current study, we classified patients into two molecular subclasses based on our evaluation of 41 GRGs' performance in ccRCC and healthy tissues. There were notable variations between the two subtypes in terms of immune infiltrating cells and clinical findings. Furthermore, there is a considerable correlation between the immunological and tumor-related pathways and both subtypes.

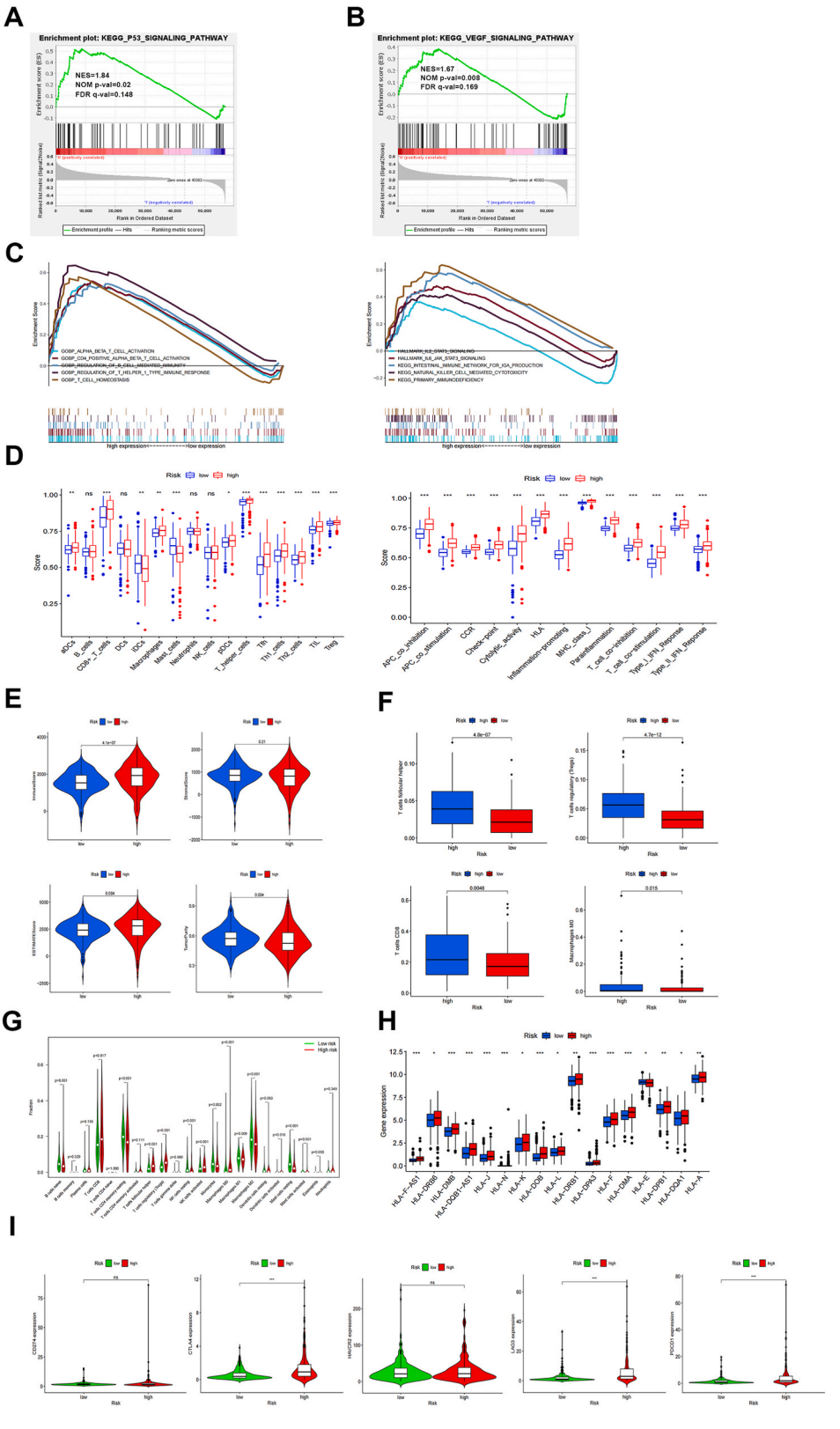

(caption on next page)

Fig. 4. | The high-risk group enriched in pathways associated with tumor formation and progression. Signaling pathways for P53 (A) and VEGF (B) were considerably enriched in the high-risk group. (C) Increase the number of pathways linked to immunological, chemokine, and MHC molecules enriched in the high-risk group. Immune cell infiltration and immune-related functions or pathways (D), immune and stromal scores (E), immune cell infiltration using TIMER (F) and CIBERSORT (G), MHC molecules expression level (H), five common immunoinhibitors (I) between the high- and low-risk groups. (*P < 0.05; **P < 0.01; ***P < 0.001; ns, not significant).

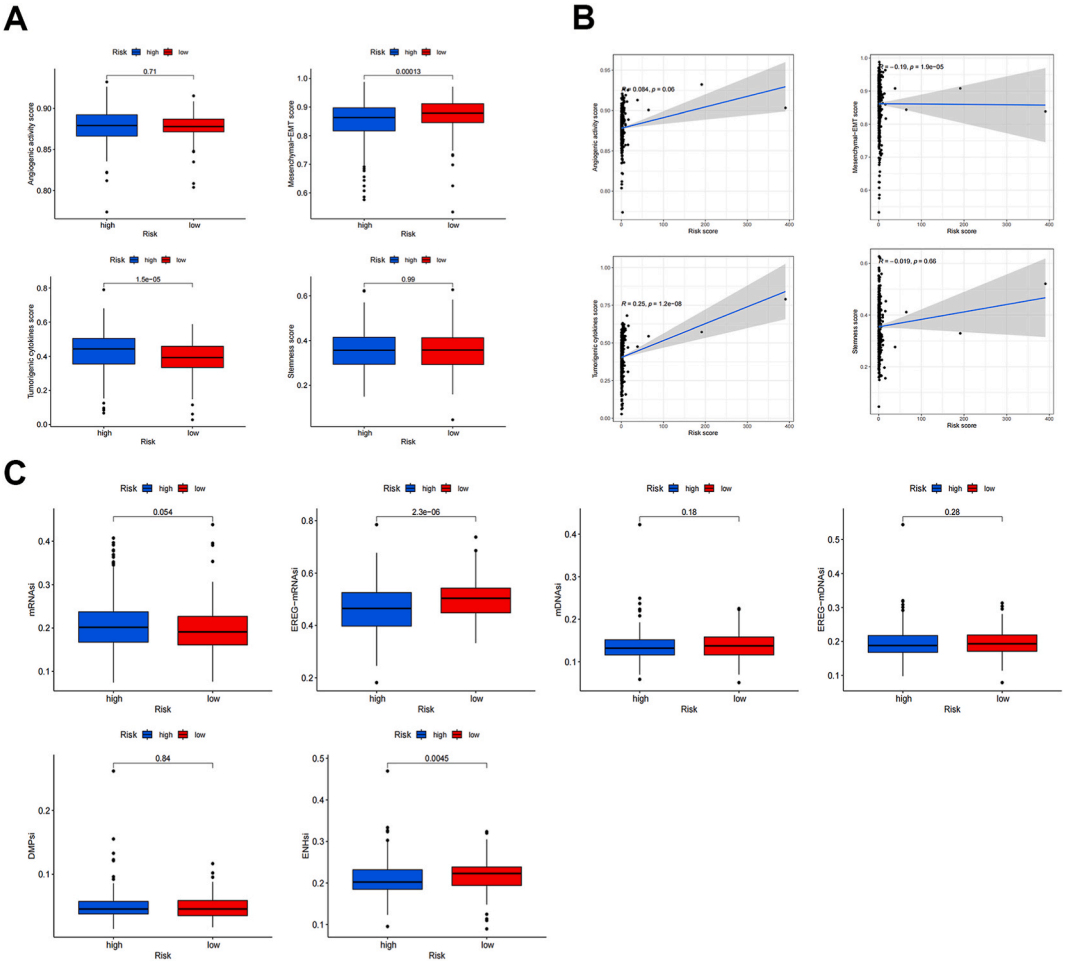

Fig. 5. | (A) Differences between the high- and low-risk groups in terms of angiogenic activity, mesenchymal-EMT, tumourigenic cytokines, and stemness scores. (B) The relationship between the risk score, mesenchymal-EMT, tumour-promoting cytokines, and stemness scores. TSI variations between the two groups (C). TSIs, Tumour stemness indices. (*P < 0.05; **P < 0.01; ***P < 0.001; ns, not significant).

We then built quantitative nomograms and robust prognostic models for GRGs, which greatly enhanced their performance. Clinical features, prognosis, tumor microenvironment (TME), immune checkpoint expression, mutation spectrum, responsiveness to immunotherapy, and medication sensitivity were all significantly different between the high and low GRG score groups. Prognostic models based on GRGs can show the effectiveness of various treatments and enable more accurate prognostication and classification of patients, which is crucial in clinical practice.

We discovered that these 16 genes were somewhat related to cancers after reviewing the literature. 13 genes linked explicitly to ccRCC were found among them, according to the research found in PubMed. For instance, the predictive biomarker ST3GAL5 has been linked to CD8 + T-cell depletion in ccRCC [21]. A poor prognosis for ccRCC can result from high PLAUR expression [22]. LGALS1 can predict probable immunological checkpoints and the effectiveness of anti-PD1 treatment in ccRCC patients [23]. In patients with ccRCC, overexpression of NEIL3 is linked to poor survival [24]. In individuals with ccRCC, CDH13 has been identified as a possible therapeutic target [25]. Regarding renal clear cell carcinoma, CSF2, TLR3, and RNASE2 closely correlate with immune infiltration and predict overall survival [15,16,26]. TIMP1 can hasten the development of renal clear cell carcinoma 21 through the EMT signaling pathway [27]. Patients treated for renal cell carcinoma with sunitinib in the first line may benefit from using KDR as a predictive biomarker of clinical outcome [28]. According to reports, LY96 may target dendritic cells in immunotherapy for renal cell carcinoma [29]. In clear cell renal cell carcinoma, TEK is a new prognostic marker [30]. Clear cell renal cell carcinoma's clinicopathological

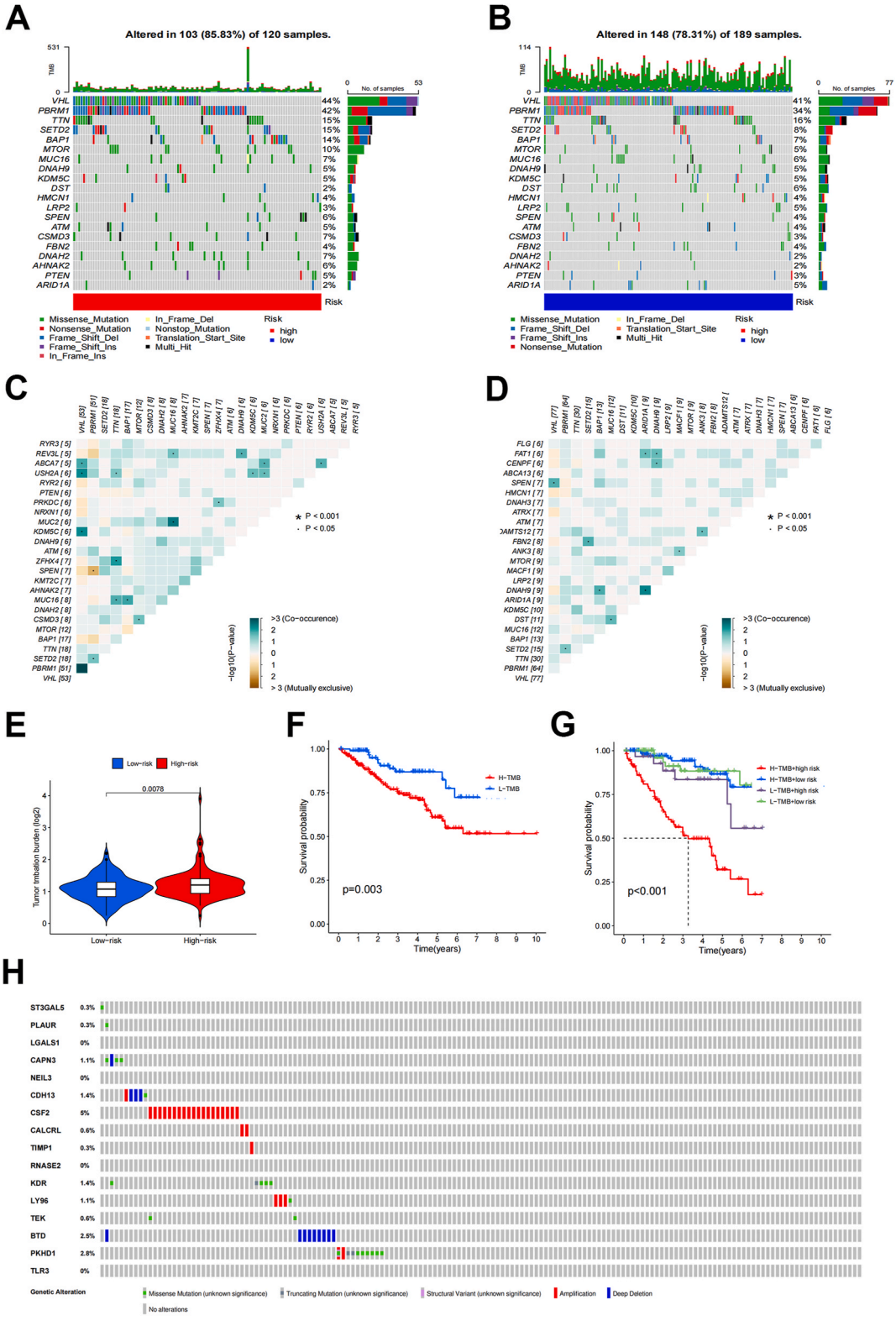

(caption on next page)

Fig. 6. | The somatic mutations in the high-risk group (A) and the low-risk group are depicted in waterfall maps (B). Heatmap shows the mutually exclusive mutations and co-occurrences of the variously altered genes in the high-risk group (C) and the low-risk group (D). *p < 0.01. (E) TMB comparison between groups at high and low risk. (F) A distinction in overall survival between groups with high and low TMB levels. Based on TMB and risk score, there is a difference in overall survival (G). (H) The 16 gene mutation rates in ccRCC patients as reported by the cBioPortal database. (ns, not significant).

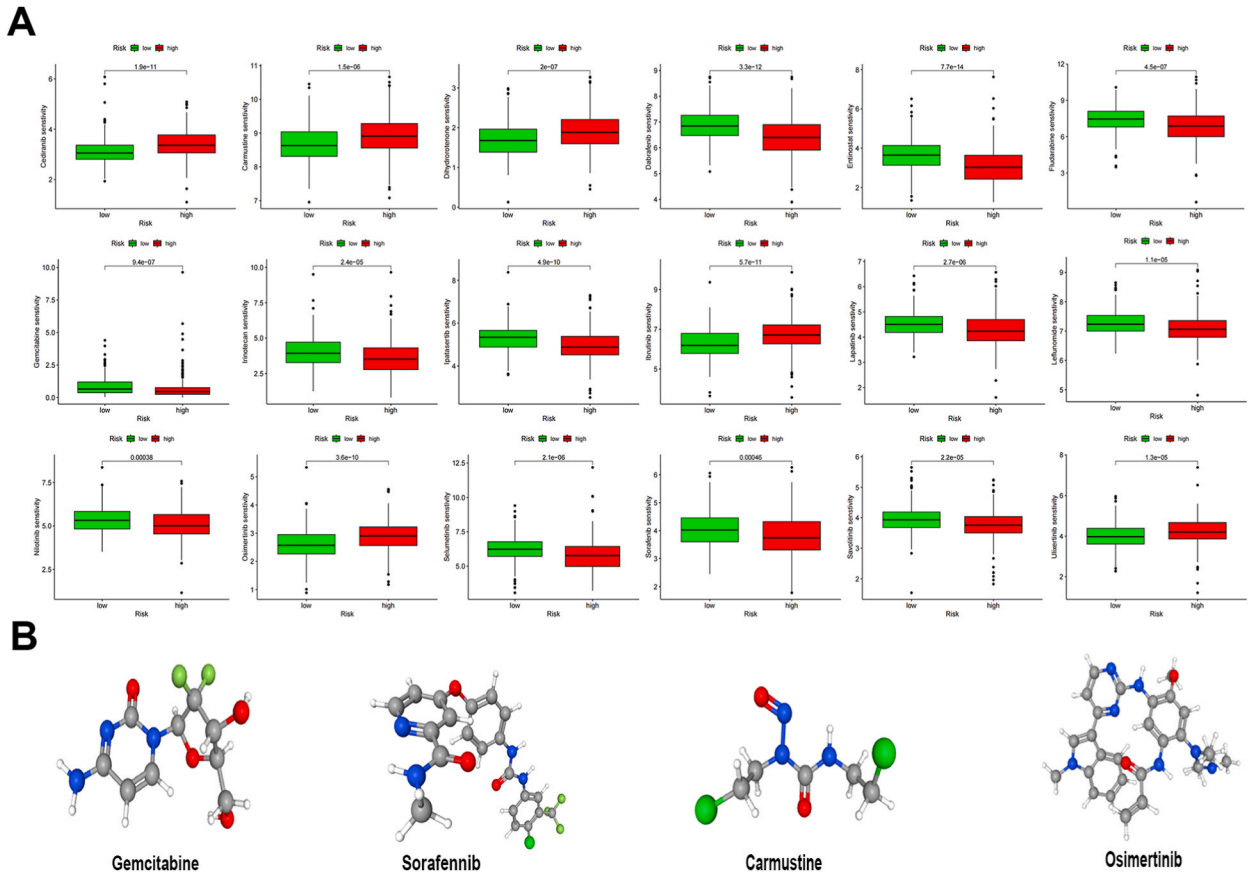

Fig. 7. | (A) The dissimilarities between high- and low-risk patients' reactions to standard chemotherapy medicines. (B) Four probable target medicines' 3D structures. (*P < 0.05; **P < 0.01; ***P < 0.001; NS, not significant).

characteristics and prognosis are linked to the m6A-related immunity gene PKHD1 [31]. A PubMed search for "GENE and ccRCC" revealed that three genes (CAPN3, CALCRL, and BTD) had not been examined concerning ccRCC. More fundamental and clinical investigations are necessary to confirm our findings, the processes underlying the predictive significance of the 16 genes on which GRGs are based, and develop new therapeutic targets to extend OS in ccRCC patients.

There is a tight relationship between immune infiltration and the clinical prognosis of renal cell carcinoma (RCC). The most recent theory states that the amount and distribution of invading immune cells are critical factors in cancer development, immunotherapy efficacy, and prognosis. Tumor-infiltrating immune cells (TICs) may have predictive value as they create a mini-ecosystem in the cancer microenvironment [32]. The phenotypic and operation of tumor cells can be interfered with by efficient immune responses in the tumor microenvironment. The association between glycosylation processes and the tumor microenvironment further clarifies the link between immune infiltrates and risk groups. We discovered several disparities in immune cell infiltration in numerous low- and high-risk groups using the glycosylation-related gene signature. We discovered that the high-risk group had higher levels of CD8 + T, macrophages, and Treg expression, which may account for the variations in prognosis between the high-risk and low-risk groups. Growing data shows that individuals with ccRCC who have higher amounts of three cells would have a poorer prognosis [33–37]. Further, we found a significant increase in the prevalence of M0 macrophages and mast cells in the high-risk group. M0 macrophages can become M2 macrophages, promoting immune evasion [38]. In addition, mast cells play a crucial role in controlling inflammation and immunosuppression [39]. In addition to suppressing immune responses against tumors by releasing anti-inflammatory cytokines, they can also promote tumor growth by controlling the formation of new blood vessels [40,41]. The high-risk subgroup showed increased immune cells infiltrating the tumor, leading to their classification as "hot tumors," which may be responsible for the significantly poorer survival of high-risk ccRCC patients, which suggests excellent potential for anti-cancer. Additionally, Type II IFN

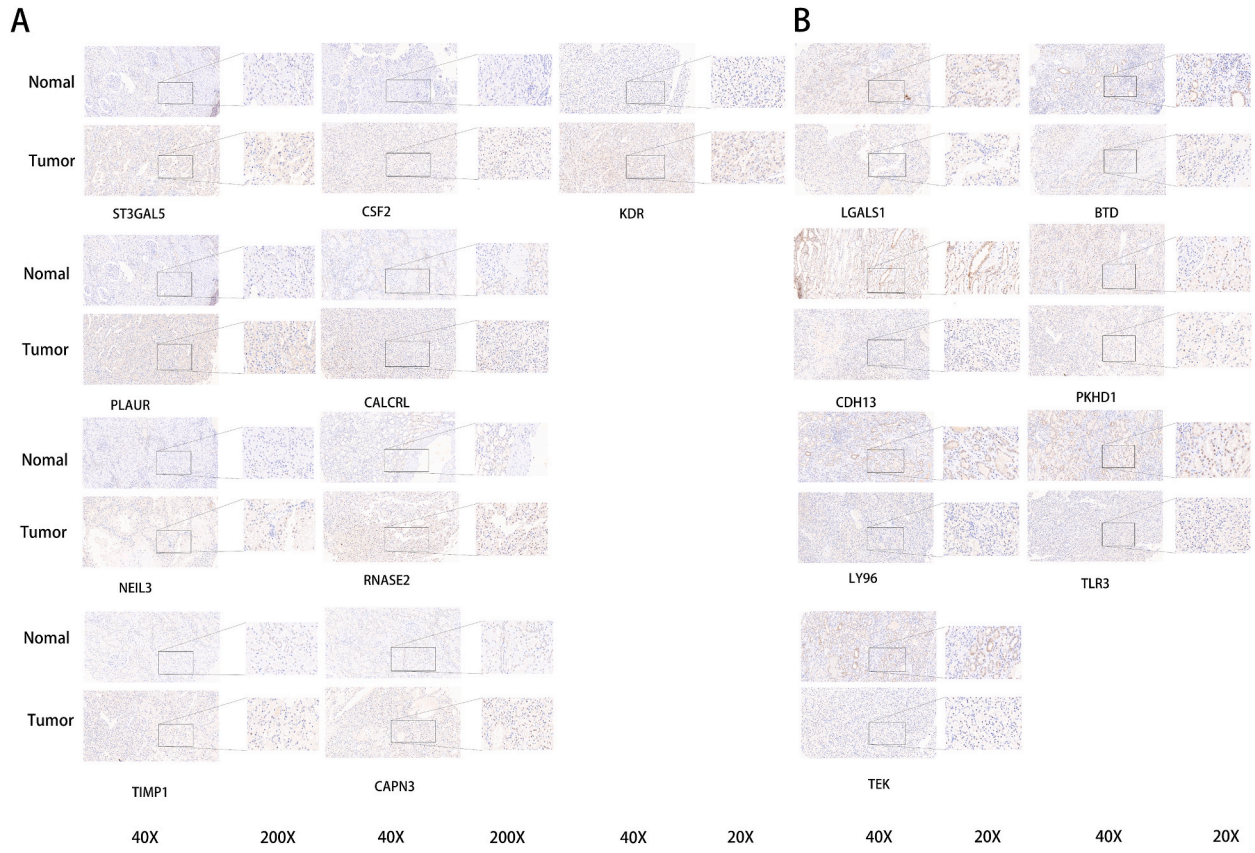

Fig. 8. | IHC analysis of model genes. (A) Genes are highly expressed in renal cancer tissues compared to adjacent non-cancerous tissues. (B) Genes are highly expressed in adjacent non-cancerous tissues compared to renal cancer tissues.

Response expression, which is thought to be a crucial component in coordinating the interaction between malignancies and the immune system, was much more significant in the high-risk group than in the low-risk group [42]. As a result of suppressing CTLA-4, GPC3, PDCD1, and PDL1, immune checkpoint drugs have demonstrated new potential in treating cancer [43]. According to our research, the high-risk group had higher CTLA4, PDCD1, and LAG3 expression levels. As a result, immunotherapy may work for patients who express immune checkpoint inhibitors highly. Renal cell carcinoma has responded well to PD-1 and CTLA-4 targeted immunotherapy in combination with nivolumab and ipilimumab [44]. The elevated expression of immune checkpoints and the tumor's immunological microenvironment activity are consistent with these findings. The tumor immune milieu may thus be reliably assessed using this signature, and the effectiveness of immune checkpoint inhibitors can be predicted.

There is evidence linking TMB to both immunotherapy response and clinical outcome. According to several studies, TMB strongly predicts progression-free survival and objective response rate; overall survival is only partially predicted by raised TMB [45]. Our investigation revealed a significant relationship between TMB and GRG model scores. By integrating TMB and score into an all-inclusive predictive model, we enhanced the prognosis for survival and thus offered significant insights for guiding immunotherapy. The effectiveness of immunotherapy as a crucial clinical strategy for cancer treatment has significantly increased due to the success of immune checkpoint inhibition. Clinical investigations have verified the safety and effectiveness of various ICIs [46,47]. Our survey showed notable variations in immune checkpoint performance across rating categories; this is a valuable point of reference for further immunotherapy.

Immunophenotype-based stratification is effective, and our created prognostic profile is immune by nature. Our simulations of the effects of various medications on various reactions also showed how significantly the sensitivity to multiple treatments varied between the high-risk and low-risk groups. We will examine the connection between these medications and renal clear cell carcinoma throughout upcoming investigations. We further validated the expression of model genes, and we performed immunohistochemical experiments on clinically operated ccRCC tissue and adjacent non-cancerous tissue specimens. We observed 16 model genes, which are consistent with our Shengxin analysis results. Further experiments are needed in the future to validate functional differences in individual model genes.

However, we must acknowledge that there are some inevitable limitations to our study. Our study is mainly based on a public database of bioinformatics approaches, and more in vivo and in vitro studies are needed to determine how these 16 identified genes contribute to the formation of ccRCC patients. Second, due to the lack of complete patient survival data in external datasets, GSE29609

used in the current study as external validation requires the inclusion of more datasets containing survival data for validation in the future due to the small amount of data. In addition, the risk model only examined immune cells, immune function, MHC molecules, immune checkpoints, and immunotherapy in this study. Potential links between risk models and immune status are only suggestive. We will continue to collect sufficient samples in the future to assess the usefulness of this model in combination with immunotherapy and to see if there is a difference in the benefit of immunotherapy between the high-risk and low-risk groups. Finally, the fact that people's responses to different drugs can vary widely impacts the time and effort we devote to studying new treatment options.

4. Conclusion

In conclusion, our work uses GRGs to create predictive profiles and molecular subtypes of renal clear cell carcinoma. In addition, differences in immune patterns, gene mutation status, and drug sensitivity between various molecular subtypes and risk groups were examined. This feature helps to optimize individualized treatment, making it invaluable for clinical application and translation.

5. Materials and methods

5.1. Clinical patients and tissue samples

The Second Affiliated Hospital of Nantong University gathered 43 paired RCC tissue samples and adjacent non-cancerous samples from patients undergoing radical or partial nephrectomy between 2017 and 2019 and compared them to their normal tissue counterparts. Following collection, the tissue samples were put into immediate storage at −80 °C. This study has received unanimous approval (Ethics No. 2021YL012) from the Second Affiliated Hospital's ethics committee by the 1964 Helsinki Declaration. All participants' patients received thorough explanations and signed written informed consent forms.

5.2. Acquisition of data

We obtained information about simple nucleotide variations, pertinent clinical data, and RNA-seq data from the TCGA website (https://portal.gdc.cancer.gov/). GSE29609 is the dataset that was downloaded from the GEO database (https://www.ncbi.nlm.nih.gov/geo/). Using the GEOquery program in R, the gene expression and clinical datasets were retrieved. The clinical data collection was analyzed to gather information on grade, T, M, and N as well as survival time and status. The sample size was 39 instances after integrating the clinical data by sample name with the GEO transcriptome data. 39 samples from GSE29609 were approved as a test set for judging prognostic model precision. All patient files with missing data were removed. 1005 glycosylation genes were extracted from GeneCards (https://www.genecards.org) with a relevance score $\geq$7.

5.3. Differential expression analysis of glycosylation-related genes (DE-GRGs)

When comparing 72 normal renal tissues and 539 ccRCC tissues from the TCGA, DE-GRGs were generated using a screening threshold of $|\log \text{Foldchange (FC)}| > 1$ and a false discovery rate (FDR) of 0.05. The Kyoto Encyclopedia of Genes and Genomes and Gene Ontology (GO) were then analyzed using DE-GRGs (KEGG). Cytoscape and the STRING database were used to examine protein-protein interactions (PPIs). Cytohubba and MCODE plugins examined hub genes and modules.

5.4. Cluster analysis

The identification of 41 DE-GRGs linked to prognosis was done using a single-variable Cox regression analysis (Supplementary table 2). The "ConsensusClusterPlus" program was used to conduct a cluster analysis to determine the various molecular subtypes linked with glycosylation. To compare outcomes between the two groups, we employed Kaplan-Meier (K-M) analysis. Chi-square tests were used for research, and heat maps were produced to display the relationship between clustering and clinical characteristics.

5.5. Generation of the prognostic model

To identify independent genes for ccRCC and create prognostic characteristics, multivariate Cox regression analysis was also performed. Graphpad software displayed the coefficients of chosen genes. The predictive value of the attributes was assessed using K-M analysis and receiver operating characteristic (ROC) curves. We tested whether or not the signature was an independent risk factor using univariate and multivariate Cox analysis. Correlation analysis, stratified analysis, and nomogram building between risk score and clinical features were performed by clinicopathologic criteria. Calibration plots were used for 1-, 3-, and 5-year survival to assess the degree of agreement between projected probability and actual survival.

5.6. Immunohistochemistry (IHC)

We tested IHC on the retrieved RCC and the nearby normal tissues. The paraffin tissue sections were deparaffinized in xylene and then submerged in graded alcohol solutions for hydration after baking at 60 °C for 60 min. After applying a drop of Ultra V Block to the slides to block them for 5 min, tissue slices were incubated with a primary anti-gene antibody (1:100–1:1000, Proteintech) overnight at

4 °C. The anti-rabbit/mouse IgG (1:200–1:500, Proteintech) secondary antibody was added dropwise to the slides after they had been cleaned with PBS. The slides were then incubated at 37 °C for 10–30 min. Before being examined under a microscope, the tissue samples were finally dyed with diaminobenzidine (DAB).

5.7. Feature-based gene set enrichment analysis

In order to investigate probable processes, we employed GSEA to examine route enrichment in the high-risk group. There were four genes in the internal reference gene set: c2kegg, c2biocartar, and c5go. Normalized enrichment score (NES) > 1, nominal (NOM) p-value <0.05, and FDR q-value <0.25 were the screening criteria.

5.8. Immunologic Landscape analysis

The immunological state of high-risk and low-risk groups was compared using three immune-related algorithms. Each sample's immune cell activity, immunological function, and immune route were determined using one-sample GSEA (ssGSEA). From earlier research, marker genes for various immune cells were developed. The ESTIMATE method was used to determine the immune score, stromal score, projected score, and tumor purity based on the ratio of immune cells to stromal cells. The CIBERSORT algorithm predicted the makeup of immune cells that infiltrated each tumor sample. Based on cluster analysis and characterization, we also compared MHC molecule expression.

The clustering and danger of five popular immunosuppressive molecules (PD-L1, CTLA4, HAVCR2, LAG3, and PD1) were first studied regarding immune checkpoints. Longer survival and worse resistance checkpoint blockade therapy are well-known to be associated with higher tumor immune dysfunction and rejection (TIDE) scores. Physicians can choose patients who will benefit more from immune checkpoint treatment using the TIDE score. As a result, using the TIDE database, we generated the TIDE score for TCGA ccRCC patients.

5.9. Analysis of tumor-related scores and tumor stemness indices (TSIs)

In earlier research, it was discovered that individuals with a poor prognosis for glioma had higher scores for angiogenic activity, mesenchymal epithelial-mesenchymal transition (EMT), tumorigenic cytokine, and stemness. We used the ssGSEA method to determine scores for each tumor sample for angiogenic activity, mesenchymal-EMT, Tumorigenic cytokines score, and stemness. Biological activity and a greater level of tumor dedifferentiation in stem cells are linked to TSIs. We got TSIs from TCGA patients from a previous study [48].

5.10. Gene mutation analysis

We used the "maftools" software to execute gene mutations based on TCGA somatic mutation data. The tumor mutation burden (TMB) was then determined for each patient and contrasted between the high-risk and low-risk groups. TMB score was used to do a survival analysis. The cBioPortal database displayed somatic mutations in a few of the signature's chosen genes.

5.11. Chemotherapy response

We used the Genomics of Drug Sensitivity in Cancer (GDSC) database, a public dataset combining cancer cell drug sensitivity information and molecular markers of drug response [49], to evaluate the impact of predictive characteristics in predicting ccRCC treatment response. The oncoPredict package [50] was used to download the gene expression profiles for the GDSC2 gene and data regarding associated drug responses. The half maximum inhibitory concentration (IC50) of all medications in ccRCC patients was predicted using sensitivity ratings.

Data availability

Data used to support the conclusions of this investigation, including expression and clinical information, have been placed in the TCGA repository (https://portal.gdc.cancer.gov/), and GEO repository (https://www.ncbi.nlm.nih.gov/geo/) All of the aforementioned databases allow users to obtain their data for free, and our research complied with their terms of service.

Funding

The present study was supported by the Medical Research Project of Nantong Health Commission (MS2022017), Jiangsu Health Commission (Z2022014), Nantong Science and Technology Bureau (MS22019009), Youth Project of Health Commission of Nantong City (QN2022017), Social and People's Livelihood Project (MS22022085) and Nantong Science and Technology Bureau (MSZ2022101).

Ethics approval

The Second Affiliated Hospital of Nantong University (Nantong, China) Ethics Committee approved the human investigations (approval number. 2021YL012) by the 1964 Declaration of Helsinki. Every patient who took part gave their informed consent in writing.

Consent for publication

The authors declare that they consent for publication.

CRediT authorship contribution statement

Cheng Shen: Writing – original draft, Resources, Methodology, Data curation, Conceptualization. **Bing Zheng:** Software, Formal analysis, Data curation, Conceptualization. **Zhan Chen:** Software, Methodology, Investigation, Funding acquisition. **Wei Zhang:** Validation, Supervision, Software, Formal analysis, Data curation. **Xinfeng Chen:** Methodology, Funding acquisition, Formal analysis, Data curation. **Siyang Xu:** Supervision, Project administration, Methodology, Investigation. **Jianfeng Ji:** Software, Resources, Project administration, Data curation. **Xingxing Fang:** Visualization, Validation, Supervision, Software, Resources. **Chunmei Shi:** Writing – review & editing, Writing – original draft, Visualization, Funding acquisition, Data curation.

Declaration of competing interest

The authors declare that they have no known competing financial interests or personal relationships that could have appeared to influence the work reported in this paper.

Acknowledgements

The authors are grateful for the help of all colleagues and the public database.

Appendix A. Supplementary data

Supplementary data to this article can be found online at https://doi.org/10.1016/j.heliyon.2024.e27710.

References

[1] K.D. Miller, L. Nogueira, A.B. Mariotto, J.H. Rowland, K.R. Yabroff, C.M. Alfano, A. Jemal, J.L. Kramer, R.L. Siegel, Cancer treatment and survivorship statistics, CA A Cancer J. Clin. 69 (2019) 363–385, https://doi.org/10.3322/caac.21565, 2019.
[2] S. Fernández-Pello, F. Hofmann, R. Tahbaz, L. Marconi, T.B. Lam, L. Albiges, K. Bensalah, S.E. Canfield, S. Dabestani, R.H. Giles, M. Hora, M.A. Kuczyk, A. S. Merseburger, T. Powles, M. Staehler, A. Volpe, B. Ljungberg, A. Bex, A Systematic review and Meta-analysis comparing the effectiveness and Adverse effects of different systemic treatments for non-clear cell renal cell carcinoma, Eur. Urol. 71 (2017) 426–436, https://doi.org/10.1016/j.eururo.2016.11.020.
[3] C. Gao, X. Guo, A. Xue, Y. Ruan, H. Wang, X. Gao, High intratumoral expression of eIF4A1 promotes epithelial-to-mesenchymal transition and predicts unfavorable prognosis in gastric cancer, Acta Biochim. Biophys. Sin. 52 (2020) 310–319, https://doi.org/10.1093/abbs/gmz168.
[4] M. Vacante, A.M. Borzì, F. Basile, A. Biondi, Biomarkers in colorectal cancer: current clinical utility and future perspectives, World J Clin Cases 6 (2018) 869–881, https://doi.org/10.12998/wjcc.v6.i15.869.
[5] E. Koncina, S. Haan, S. Rauh, E. Letellier, Prognostic and predictive molecular biomarkers for colorectal cancer: Updates and Challenges, Cancers 12 (2020) 319, https://doi.org/10.3390/cancers12020319.
[6] M. Schmitt, F.R. Greten, The inflammatory pathogenesis of colorectal cancer, Nat. Rev. Immunol. 21 (2021) 653–667, https://doi.org/10.1038/s41577-021-00534-x.
[7] S.S. Pinho, C.A. Reis, Glycosylation in cancer: mechanisms and clinical implications, Nat. Rev. Cancer 15 (2015) 540–555, https://doi.org/10.1038/nrc3982.
[8] K.B. Chandler, C.E. Costello, N. Rahimi, Glycosylation in the tumor microenvironment: implications for tumor angiogenesis and metastasis, Cells 8 (2019) 544, https://doi.org/10.3390/cells8060544.
[9] L. Jia, J. Li, P. Li, D. Liu, J. Li, J. Shen, B. Zhu, C. Ma, T. Zhao, R. Lan, L. Dang, W. Li, S. Sun, Site-specific glycoproteomic analysis revealing increased core-fucosylation on FOLR1 enhances folate uptake capacity of HCC cells to promote EMT, Theranostics 11 (2021) 6905–6921, https://doi.org/10.7150/thno.56882.
[10] L. Chen, Y. Ling, H. Yang, Comprehensive analysis of the potential prognostic value of 11 glycosylation-related genes in head and neck squamous cell carcinoma and their correlation with PD-L1 expression and immune infiltration, J Oncol 2022 (2022) 2786680, https://doi.org/10.1155/2022/2786680.
[11] P. Ahluwalia, R. Kolhe, G.K. Gahlay, The clinical relevance of gene expression based prognostic signatures in colorectal cancer, Biochim. Biophys. Acta Rev. Canc 1875 (2021) 188513, https://doi.org/10.1016/j.bbcan.2021.188513.
[12] L. Zhang, L. Di, J. Liu, X. Lei, M. Gu, W. Zhang, Y. Wang, The LncRNA signature associated with cuproptosis as a novel biomarker of prognosis in immunotherapy and drug screening for clear cell renal cell carcinoma, Front. Genet. 14 (2023) 1039813, https://doi.org/10.3389/fgene.2023.1039813.
[13] Y. Wang, J. Liu, L. Zhang, Y. Li, A predictive model based on pyroptosis-related gene features can effectively predict clear cell renal cell carcinoma prognosis and may Be an underlying target for immunotherapy, Dis. Markers 2022 (2022) 6402599, https://doi.org/10.1155/2022/6402599.
[14] X. Zhang, X. Qin, T. Yu, K. Wang, Y. Chen, Q. Xing, Chromatin regulators-related lncRNA signature predicting the prognosis of kidney renal clear cell carcinoma and its relationship with immune microenvironment: a study based on bioinformatics and experimental validation, Front. Genet. 13 (2022) 974726, https://doi.org/10.3389/fgene.2022.974726.
[15] Q. Xing, Jiaochen Luan, Shouyong Liu, Limin Ma, Y. Wang, Six RNA binding proteins (RBPs) related prognostic model predicts overall survival for clear cell renal cell carcinoma and it is associated with immune infiltration, Bosn. J. Basic Med. Sci. (2021), https://doi.org/10.17305/bjbms.2021.6097.

[16] Y. Wang, Y. Chen, B. Zhu, L. Ma, Q. Xing, A novel nine Apoptosis-related genes signature predicting overall survival for kidney renal clear cell carcinoma and its associations with immune infiltration, Front. Mol. Biosci. 8 (2021) 567730, https://doi.org/10.3389/fmolb.2021.567730.
[17] Q. Xing, T. Zeng, S. Liu, H. Cheng, L. Ma, Y. Wang, A novel 10 glycolysis-related genes signature could predict overall survival for clear cell renal cell carcinoma, BMC Cancer 21 (2021) 381, https://doi.org/10.1186/s12885-021-08111-0.
[18] J.A. Joyce, J.W. Pollard, Microenvironmental regulation of metastasis, Nat. Rev. Cancer 9 (2009) 239–252, https://doi.org/10.1038/nrc2618.
[19] Y. Zhang, H. Lai, B. Tang, Abnormal expression and prognosis value of COG Complex Members in kidney renal clear cell carcinoma (KIRC), Dis. Markers 2021 (2021) 1–23, https://doi.org/10.1155/2021/4570235.
[20] X. Zhu, A. Al-Danakh, L. Zhang, X. Sun, Y. Jian, H. Wu, D. Feng, S. Wang, D. Yang, Glycosylation in renal cell carcinoma: mechanisms and clinical implications, Cells 11 (2022) 2598, https://doi.org/10.3390/cells11162598.
[21] J. Liu, M. Li, J. Wu, Q. Qi, Y. Li, S. Wang, S. Liang, Y. Zhang, Z. Zhu, R. Huang, J. Yan, R. Zhu, Identification of ST3GAL5 as a prognostic biomarker correlating with CD8+ T cell exhaustion in clear cell renal cell carcinoma, Front. Immunol. 13 (2022) 979605, https://doi.org/10.3389/fimmu.2022.979605.
[22] Z. Wang, K. Wang, X. Gao, Z. Liu, Z. Xing, Comprehensive analysis of the importance of PLAUR in the progression and immune microenvironment of renal clear cell carcinoma, PLoS One 17 (2022) e0269595, https://doi.org/10.1371/journal.pone.0269595.
[23] Y. Li, S. Yang, H. Yue, D. Yuan, L. Li, J. Zhao, L. Zhao, Unraveling LGALS1 as a potential immune checkpoint and a predictor of the response to anti-PD1 therapy in clear cell renal carcinoma, Pathol. Oncol. Res. 26 (2020) 1451–1458, https://doi.org/10.1007/s12253-019-00710-4.
[24] O.T. Tran, S. Tadesse, C. Chu, D. Kidane, Overexpression of NEIL3 associated with altered genome and poor survival in selected types of human cancer, Tumour Biol 42 (2020) 1010428320918404, https://doi.org/10.1177/1010428320918404.
[25] Y. Shao, W. Li, L. Zhang, B. Xue, Y. Chen, Z. Zhang, D. Wang, B. Wu, CDH13 is a prognostic biomarker and a potential therapeutic target for patients with clear cell renal cell carcinoma, Am. J. Cancer Res. 12 (2022) 4520–4544.
[26] G. Liao, J. Lv, A. Ji, S. Meng, C. Chen, TLR3 Serves as a prognostic biomarker and Associates with immune infiltration in the renal clear cell carcinoma microenvironment, J Oncol 2021 (2021) 3336770, https://doi.org/10.1155/2021/3336770.
[27] Y. Shou, Y. Liu, J. Xu, J. Liu, T. Xu, J. Tong, L. Liu, Y. Hou, D. Liu, H. Yang, G. Cheng, X. Zhang, TIMP1 indicates poor prognosis of renal cell carcinoma and accelerates tumorigenesis via EMT signaling pathway, Front. Genet. 13 (2022) 648134, https://doi.org/10.3389/fgene.2022.648134.
[28] L. del Puerto-Nevado, F. Rojo, S. Zazo, C. Caramés, G. Rubio, R. Vega, C. Chamizo, V. Casado, J. Martínez-Useros, R. Rincón, M. Rodríguez-Remírez, A. Borrero-Palacios, I. Cristóbal, J. Madoz-Gúrpide, O. Aguilera, J. García-Foncillas, Active angiogenesis in metastatic renal cell carcinoma predicts clinical benefit to sunitinib-based therapy, Br. J. Cancer 110 (2014) 2700–2707, https://doi.org/10.1038/bjc.2014.225.
[29] G. Fang, X. Wang, Prognosis-related genes participate in immunotherapy of renal clear cell carcinoma possibly by targeting dendritic cells, Front. Cell Dev. Biol. 10 (2022) 892616, https://doi.org/10.3389/fcell.2022.892616.
[30] M. Ha, Y.R. Son, J. Kim, S.M. Park, C.M. Hong, D. Choi, W. Kang, J.H. Kim, K.J. Lee, D. Park, M.E. Han, S.O. Oh, D. Lee, Y.H. Kim, TEK is a novel prognostic marker for clear cell renal cell carcinoma, Eur. Rev. Med. Pharmacol. Sci. 23 (2019) 1451–1458, https://doi.org/10.26355/eurrev_201902_17102.
[31] Z. Huang, W. Kang, Q. Zhang, N6-methyladenosine methylation related immune biomarkers correlates with clinicopathological characteristics and prognosis in clear cell renal cell carcinoma, Transl. Cancer Res. 11 (2022) 1576–1586, https://doi.org/10.21037/tcr-21-1953.
[32] S.I. Grivennikov, F.R. Greten, M. Karin, Immunity, inflammation, and cancer, Cell 140 (2010) 883–899, https://doi.org/10.1016/j.cell.2010.01.025.
[33] E.J. Wherry, M. Kurachi, Molecular and cellular insights into T cell exhaustion, Nat. Rev. Immunol. 15 (2015) 486–499, https://doi.org/10.1038/nri3862.
[34] D.E. Speiser, P.-C. Ho, G. Verdeil, Regulatory circuits of T cell function in cancer, Nat. Rev. Immunol. 16 (2016) 599–611, https://doi.org/10.1038/nri.2016.80.
[35] S. Santagata, M. Napolitano, C. D'Alterio, S. Desicato, S.D. Maro, L. Marinelli, A. Fragale, M. Buoncervello, F. Persico, L. Gabriele, E. Novellino, N. Longo, S. Pignata, S. Perdonà, S. Scala, Targeting CXCR4 reverts the suppressive activity of T-regulatory cells in renal cancer, Oncotarget 8 (2017) 77110, https://doi.org/10.18632/oncotarget.20363. –77120.
[36] Y. Qi, Y. Xia, Z. Lin, Y. Qu, Y. Qi, Y. Chen, Q. Zhou, H. Zeng, J. Wang, Y. Chang, Q. Bai, Y. Wang, Y. Zhu, L. Xu, L. Chen, Y. Kong, W. Zhang, B. Dai, L. Liu, J. Guo, J. Xu, Tumor-infiltrating CD39+CD8+ T cells determine poor prognosis and immune evasion in clear cell renal cell carcinoma patients, Cancer Immunol. Immunother. 69 (2020) 1565–1576, https://doi.org/10.1007/s00262-020-02563-2.
[37] H. Zhang, G. Zhu, Beyond promoter: the role of macrophage in invasion and progression of renal cell carcinoma, Curr. Stem Cell Res. Ther. 15 (2020) 588–596, https://doi.org/10.2174/1574888X15666200225093210.
[38] M. Roulleaux Dugage, E.F. Nassif, A. Italiano, R. Bahleda, Improving immunotherapy efficacy in soft-tissue sarcomas: a biomarker driven and histotype tailored review, Front. Immunol. 12 (2021) 775761, https://doi.org/10.3389/fimmu.2021.775761.
[39] B. Huang, Z. Lei, G.-M. Zhang, D. Li, C. Song, B. Li, Y. Liu, Y. Yuan, J. Unkeless, H. Xiong, Z.-H. Feng, SCF-mediated mast cell infiltration and activation exacerbate the inflammation and immunosuppression in tumor microenvironment, Blood 112 (2008) 1269–1279, https://doi.org/10.1182/blood-2008-03-147033.
[40] G. Varricchi, M.R. Galdiero, S. Loffredo, G. Marone, R. Iannone, G. Marone, F. Granata, Are mast cells MASTers in cancer? Front. Immunol. 8 (2017) https://doi.org/10.3389/fimmu.2017.00424.
[41] Y. Xiong, L. Liu, Y. Xia, Y. Qi, Y. Chen, L. Chen, P. Zhang, Y. Kong, Y. Qu, Z. Wang, Z. Lin, X. Chen, Z. Xiang, J. Wang, Q. Bai, W. Zhang, Y. Yang, J. Guo, J. Xu, Tumor infiltrating mast cells determine oncogenic HIF-2α-conferred immune evasion in clear cell renal cell carcinoma, Cancer Immunol. Immunother. 68 (2019) 731–741, https://doi.org/10.1007/s00262-019-02314-y.
[42] G.P. Dunn, C.M. Koebel, R.D. Schreiber, Interferons, immunity and cancer immunoediting, Nat. Rev. Immunol. 6 (2006) 836–848, https://doi.org/10.1038/nri1961.
[43] J. Qu, M. Jiang, L. Wang, D. Zhao, K. Qin, Y. Wang, J. Tao, X. Zhang, Mechanism and potential predictive biomarkers of immune checkpoint inhibitors in NSCLC, Biomed. Pharmacother. 127 (2020) 109996, https://doi.org/10.1016/j.biopha.2020.109996.
[44] E. Perez-Ruiz, L. Minute, I. Otano, M. Alvarez, M.C. Ochoa, V. Belsue, C. de Andrea, M.E. Rodriguez-Ruiz, J.L. Perez-Gracia, I. Marquez-Rodas, C. Llacer, M. Alvarez, V. de Luque, C. Molina, A. Teijeira, P. Berraondo, I. Melero, Prophylactic TNF blockade uncouples efficacy and toxicity in dual CTLA-4 and PD-1 immunotherapy, Nature 569 (2019) 428–432, https://doi.org/10.1038/s41586-019-1162-y.
[45] R. Li, D. Han, J. Shi, Y. Han, P. Tan, R. Zhang, J. Li, Choosing tumor mutational burden wisely for immunotherapy: a hard road to explore, Biochim. Biophys. Acta Rev. Canc 1874 (2020) 188420, https://doi.org/10.1016/j.bbcan.2020.188420.
[46] R.S. Riley, C.H. June, R. Langer, M.J. Mitchell, Delivery technologies for cancer immunotherapy, Nat. Rev. Drug Discov. 18 (2019) 175–196, https://doi.org/10.1038/s41573-018-0006-z.
[47] Y. Zhang, Z. Zhang, The history and advances in cancer immunotherapy: understanding the characteristics of tumor-infiltrating immune cells and their therapeutic implications, Cell. Mol. Immunol. 17 (2020) 807–821, https://doi.org/10.1038/s41423-020-0488-6.
[48] T.M. Malta, A. Sokolov, A.J. Gentles, T. Burzykowski, L. Poisson, J.N. Weinstein, B. Kamińska, J. Huelsken, L. Omberg, O. Gevaert, A. Colaprico, P. Czerwińska, S. Mazurek, L. Mishra, H. Heyn, A. Krasnitz, A.K. Godwin, A.J. Lazar, J.M. Stuart, K.A. Hoadley, P.W. Laird, H. Noushmehr, M. Wiznerowicz, Machine learning identifies stemness features associated with oncogenic dedifferentiation, Cell 173 (2018) 338–354.e15, https://doi.org/10.1016/j.cell.2018.03.034.
[49] F. Iorio, T.A. Knijnenburg, D.J. Vis, G.R. Bignell, M.P. Menden, M. Schubert, N. Aben, E. Gonçalves, S. Barthorpe, H. Lightfoot, T. Cokelaer, P. Greninger, E. Van Dyk, H. Chang, H. De Silva, H. Heyn, X. Deng, R.K. Egan, Q. Liu, T. Mironenko, X. Mitropoulos, L. Richardson, J. Wang, T. Zhang, S. Moran, S. Sayols, M. Soleimani, D. Tamborero, N. Lopez-Bigas, P. Ross-Macdonald, M. Esteller, N.S. Gray, D.A. Haber, M.R. Stratton, C.H. Benes, L.F.A. Wessels, J. Saez-Rodriguez, U. McDermott, M.J. Garnett, A landscape of pharmacogenomic interactions in cancer, Cell 166 (2016) 740–754, https://doi.org/10.1016/j.cell.2016.06.017.
[50] D. Maeser, R.F. Gruener, R.S. Huang, oncoPredict: an R package for predicting *in vivo* or cancer patient drug response and biomarkers from cell line screening data, Briefings Bioinf. 22 (2021) bbab260, https://doi.org/10.1093/bib/bbab260.